^{18}F-FDG accumulation in less-affected lung area predicts postoperative interstitial lung disease acute exacerbation in lung cancer: A case control study

Kentaro Fukunaga (fukuken@belle.shiga-med.ac.jp)
Shiga Univercity of Medical Sciense https://orcid.org/0000-0002-6261-0344
Yukihiro Nagatani
Shiga University of Medical Science
Hiroaki Nakagawa
Shiga University of Medical Science
Ayumi Nitta-Seko
Shiga University of Medical Science
Tamotsu Nagata
Oumikusatsu Tokushykai Hospital
Masaki Nishizono
Shiga University of Medical Science
Kazumasa Kobashi
Shiga University of Medical Science
Harumi Iguchi
Shiga University of Medical Science
Norihisa Nitta
Shiga University of Medical Science
Jun Hanaoka
Shiga University of Medical Science
Kiyoshi Murata
Shiga University of Medical Science
Yasutaka Nakano
Shiga University of Medical Science

Research article

Keywords: interstitial lung disease, lung cancer, postoperative acute exacerbation of interstitial lung disease, 18F-flurodeoxyglucose positron emission tomography/computed tomography

Posted Date: April 7th, 2020

DOI: https://doi.org/10.21203/rs.3.rs-19006/v1

Abstract

Background: Pneumonectomy for lung cancer with interstitial lung disease (ILD) has been shown to cause postoperative acute exacerbation (AE) of the ILD. The accumulation of ^{18}F-flurodeoxyglucose (FDG) on normal parenchymal or less-affected lung fields in ^{18}F-FDG-positron emission tomography (PET)/computed tomography (CT) has been reported to be related to ILD disease activity and prognosis. To determine whether ^{18}F-FDG accumulation in normal parenchymal or less-affected lung fields on ^{18}F-FDG-PET/CT can predict postoperative AE of ILD in non-small cell lung cancer (NSCLC) patients with ILD.

Methods: This retrospective study included 36 NSCLC patients with ILD, who underwent ^{18}F-FDG-PET/CT at 2 institutions before pulmonary surgery. A single volume-of-interest (VOI) was placed to measure the mean standardized uptake value (SUV_{mean}) in normal or less-affected lung fields at 12 areas on the ventral and dorsal locations of both lungs, in each level of the aortic arch, tracheal bifurcation, and the orifice of the right lower pulmonary vein into the left atrium. The region to which the target VOI was set corresponded to no or minimally increased attenuation on high resolution CT. The SUV_{mean} was defined as the mean SUV of the target VOI, $SUV_{tissue\ fraction\ (TF)}$ as the corrected SUV_{mean} by using TF and mean computed tomography density (CTD_{mean}) as the mean attenuation of the corresponding target VOI on HRCT. We performed a phantom study to optimize SUV difference among 2 institutions. The corrected SUV_{mean} ($cSUV_{mean}$) and corrected SUV_{TF} ($cSUV_{TF}$) were calculated based on the phantom study result.

Results: Among 36 NSCLC patients with ILD who underwent pulmonary surgery, 8 patients developed postoperative AE of ILD. The $cSUV_{mean}$ values in the ventral and dorsal locations at the aortic arch level, and in the ventral location at the tracheal bifurcation level in the group with postoperative AE were higher than in the group without postoperative AE. There was no significant difference in the value of $cSUV_{TF}$ and CTD_{mean} between the groups with and without postoperative AE.

Conclusion: ^{18}F-FDG accumulation in the normal or less-affected lung fields can potentially predict postoperative AE of ILD in NSCLC patients with ILD.

Background

Interstitial lung disease (ILD) results not only from parenchymal lung diseases of known or unknown etiology, but also in lung regions with both inflammation and fibrotic changes (1, 2). ILDs are recognized as a risk factor for lung cancer (3-5). Since therapy of lung cancer, such as surgery, chemotherapy, and chemoradiotherapy sometimes provoke acute exacerbation (AE) of ILD, treatment should be chosen carefully (6-8). Pneumonectomy poses a risk of postoperative AE for patients with lung cancer-associated ILD and has a reported mortality rate between 33.3% and 100% (9-13). In a retrospective study conducted in Japan, the incidence of postoperative AE and the mortality rate in lung-cancer-associated ILD was 9.3% and high as 43.9%, respectively (13). Moreover, a high Krebs von den Lungen-6 (KL-6) value, male sex,

history of AE, preoperative steroid use, and the surgical procedure were identified as possible risk factors for postoperative AE (13).

^{18}F-flurodeoxyglucose (FDG) positron-emission tomography (PET) has been proven to be useful for the detection and follow-up of neoplastic lesions (14). Recently, several reports have stated that ^{18}F-FDG accumulation may be related to disease activity in patients with ILDs (15-17). Furthermore, increased ^{18}F-FDG uptake in apparently normal lung parenchyma on high-resolution computed tomography (HRCT) was observed in patients with idiopathic pulmonary fibrosis (IPF), and was related to the prognosis (18-20). These reports suggested that a high uptake of ^{18}F-FDG in the less-affected lung parenchyma may be an indicator of the disease activity and progression in ILD.

This retrospective study was conducted to investigate whether ^{18}F-FDG accumulation in the less-affected lung parenchyma on HRCT can predict postoperative AE in non-small cell lung cancer (NSCLC)-associated ILD.

Methods

Patient Selection

In the patient selection process, 388 patients with NSCLC who underwent pulmonary surgery in Shiga University of Medical Science between January 2011 and December 2016 were initially enrolled. Among them, 38 patients with NSCLC complicated with ILD who underwent ^{18}F-FDG PET/CT before pulmonary surgery in our hospital or Oumikusatsu Tokushukai Hospital were identified. 2 patients with glucose metabolism abnormalities were excluded. Thus, finally, 36 patients with ILD were included.

To investigate the difference in ^{18}F-FDG accumulation in the apparently normal or less-affected lung area between NSCLC patients with or without ILD, we additionally included 50 consecutive NSCLC patients without ILD who underwent both ^{18}F-FDG PET/CT before pulmonary surgery and surgery in our hospital between August 2015 and December 2016.

Available patient characteristics, clinical laboratory data, and pulmonary functional tests, including age, sex, smoking status, Eastern Cooperative Oncology Group (ECOG) performance status, histology of NSCLC, surgical procedure, stage of NSCLC, lactate dehydrogenase, C-reactive protein, krebs von den lungen-6 (KL-6), and surfactant protein-D were obtained from medical records. Whether ILD was associated with NSCLC or not was estimated by chest HRCT underwent within 3 months before pulmonary surgery. Based on HRCT image findings the NSCLC patients with ILD were classified into having the usual interstitial pneumonia (UIP) pattern and non-UIP pattern. The UIP pattern was assigned when abnormal shadows, including subpleural basal predominance, reticular abnormalities, and honeycombing with or without traction bronchiectasis were present and features of an inconsistent UIP pattern were absent, according to the International Consensus Statement of IPF(21). Otherwise, patients were diagnosed as having a non-UIP pattern.

This study was approved by our institutional review board (approved number: 29-190, November 2, 2017). The need to obtain informed patient consent was waived because of the retrospective nature of this research.

Criteria for Postoperative Exacerbation of ILD

The diagnosis of postoperative AE of ILD was based on the definition of the International Working Group Report for AE of IPF (22). The diagnostic criteria were as follows: acute worsening or development of dyspnea, typically of < 1 month duration after pulmonary surgery; new bilateral ground-glass opacity and/or consolidation on computed tomography (CT); deterioration not fully explained by cardiac failure or fluid overload (22).

PET/CT Image Data Acquisition

^{18}F-FDG PET scanning was performed using a combined PET/CT scanner (Discovery PET/CT 710, General Electronics, Fairfield, CT, USA) in our institution, or a Discovery PET/CT ST (General Electronics) in Oumikusatsu Tokushukai Hospital). All patients were instructed to fast for 5 hours or longer before ^{18}F-FDG administration. Blood glucose level was measured before ^{18}F-FDG injection to confirm a level of less than 150 mg/dL (23). Since the blood glucose level influenced ^{18}F-FDG accumulation in brain (24, 25), patients with unknown blood glucose level were excluded if accumulation of ^{18}F-FDG in their brains was judged to be insufficient. There were no cases whose blood glucose level before ^{18}F-FDG-PET imaging exceeded 150 mg/dl. However, among 10 patients for whom blood glucose level values were unavailable, 2 patients were excluded from analysis because of faint ^{18}F-FDG accumulation demonstrated in the brain. Three-dimensional PET data were acquired from the head to the thigh 60 min after the injection of a dose of 185–330 MBq/kg of ^{18}F-FDG.

High Resolution CT Image Data Acquisition

All patients underwent enhanced or un-enhanced chest HRCT by 64-row helical mode using 320-row multidetector CT scanners (Aquilion ONE, Canon Medical Systems, Otawara, Tochigi, Japan) or 16-row helical scan mode (Sensation Cardiac, Siemens, Munich, Germany) within 3 months after ^{18}F-FDG PET/CT. Other scanning parameters were as follows: tube voltage = 120 kVp, tube current; 180–320 mA (for 64-row mode) or 340–400 mA (for 16-row mode), slice thickness = 0.5 mm (for 64-row mode) and 0.75 mm (for 16-row mode), rotation time; 0.5 s (for 64-row mode) or 0.375 s (for 16-row mode); helical pitch; 40 (for 64-row mode) and 15 (for 16-row mode). CT images were reconstructed with 1-mm slice thickness, 1-mm interval, and lung kernel.

Image Analysis

PET images were analyzed on a dedicated workstation (Advantage Workstation, version 2.0; General Electronics, Fairfield, CT, USA). On PET/CT images, a single cubic target volume-of-interest (VOI) of approximately 18 cm^3 in volume (26 mm × 26 mm × 26 mm) was carefully placed to include normal-

appearing regions while avoiding the mediastinum, chest wall, central bronchus, and blood vessels, in 12 areas (Figure 1): the ventral and dorsal locations in both lungs at each of the 3 predefined levels: aortic arch (AA), tracheal bifurcation (TB), and the orifice of the right lower pulmonary vein into the left atrium (RLPV), while referring to non-increased attenuation on HRCT images. Standardized uptake values (SUVs) were defined as follows: SUV_{mean} was measured in a target VOI. SUV_{max} was measured as the highest SUV in ILD lesion (18, 19). $SUV_{tissue\ fraction\ (TF)}$ was analyzed to adjust for metabolic condition, regardless of differences in the degree of region-based aeration (26, 27). Mean CT density (CTD_{mean} on PET/CT) as well as SUV_{mean} was simultaneously obtained. CTD_{mean} on HRCT were measured using Image J (Version 1.51. National Institutes of Health, Bethesda, ML, USA), by placing an identical-sized VOI at essentially the same location where the VOI was set on PET/CT.

SUV_{mean}, SUV_{TF}, SUV_{max}, and CTD_{mean} on HRCT were independently assessed by 1 chest physician and 1 thoracic radiologist with 15 and 20 years of experience, respectively, to determine interobserver agreement.

Phantom Study for Adjustment of Measured Values between the Institutions The SUV values measured for images obtained at the 2 institutions were adjusted according to a method described in a previous study (28). Phantom experiments were performed with modification of the dedicated guideline issued by the Japan Nuclear Medicine Society, by using the National Electrical Manufacturers Association (NEMA) body phantom. The NEMA body phantom, with spherical containers of 6 different diameters: 10, 13, 17, 22, 28, and 37 mm, filled with ^{18}F-FDG, for insertion into different body parts, was scanned for 30 minutes in list-mode. The radioactivity levels were 2.65 kBq/mL for spherical containers filled with ^{18}F-FDG arranged and 0.66 KBq/mL for background parts, over 60 minutes at the time of data acquisition. SUV_{max} values of the image slice with the most highly integrated radio-isotope and the 2 antero-posterior neighboring image slices were averaged as the actual SUV_{max} for the spherical containers. The gauged mean SUV in the phantom background was determined as the mean of the SUVs of 12 ROIs of 37-mm diameter in the image slice with the most highly integrated radio-isotope and its 4 anteroposterior neighboring image slices for the 10-mm spherical container. The calibration factor was determined by dividing the actual SUV_{max} by the gauged mean SUV of the phantom background to reduce inconsistencies between 2 institutes. This adjustment for inter-institutional variability in SUV values shrunk the range from 0.69-0.89 to 0.74-0.97 when the SUV_{max} ratio was described as the SUV_{max} of the one institution to the SUV_{max} of the control institution. The original measured SUV_{max} values for both institutions were corrected by multiplication with the calibration factors derived from the phantom studies to minimize inter-institutional SUV variability; these values were defined as cSUV.

Statistical Analysis

Univariate analyses were conducted to identify the difference in geographic data, physiological parameters, and laboratory data between patients with NSCLC with ILD and without ILD, and between the NSCLC patients with and without postoperative exacerbation of ILD. All continuous and categorical

variables were analyzed with Wilcoxon's test and the chi-square test. For locations with difference in $cSUV_{mean}$, $cSUV_{TF}$, and $cSUV_{max}$ measured values based on PET/CT between NSCLC patients with and without postoperative exacerbation of ILD, receiver operating characteristic (ROC) curve analysis were performed. Two-sided P values of less than 0.05 were considered statistically significant. The normality of SUV_{mean}, SUV_{TF}, and CTD_{mean} on HRCT measured by the 2 observers was evaluated with the Shapiro–Wilk test. Inter-observer variance was evaluated by Spearman's correlation coefficient for the measured values. All statistical analyzes were performed using JMP 9.0 software (SAS Institute Inc., Cary, NC, USA).

Results

Patient Characteristics

Table E1 shows the characteristics of the NSCLC patients with ILD and those without. The median age was 73.5 years (range: 68–77 years) in NSCLC patients with ILD and 69 years (range: 63.8–72.3 years) in those without. Most NSCLC patients with ILD were men, with good ECOG performance status, and were smokers. The frequencies of adenocarcinoma and squamous cell carcinoma were higher in NSCLC patients with than in those without ILD. There was no significant difference in the surgical procedure used and stage between the 2 groups. The %VC, the %FVC, the %TLC, the DLco, and the %DLco in NCSLC patients were lower in those with than in those without ILD.

Table 1 shows the characteristics of the NSCLC patients with and without postoperative AE. Eight patients developed postoperative AE. The median duration of postoperative AE was 12 days (range: 7–32 days). The median age was 71 years (range: 66–77.3 years) in NSCLC patients with postoperative AE of ILD and 73.5 years (range: 69.3–77 years) in NSCLC patients without ILD. Most patients with postoperative AE were male, with good ECOG performance status and were smokers. There was no significant difference in histology, surgical procedure, and stage between those with and those without postoperative AE. In terms of interstitial pneumonia classification, 4 (50%) and 12 cases (43%) were diagnosed with UIP in the AE group and the non-AE group, respectively. No significant difference was found in terms of pulmonary function test parameters between the 2 groups, except for a slightly larger value of surfactant protein D in patients with postoperative AE.

Inter-observer Agreement

Values measured by the 2 observers were not all normally distributed. Spearman correlation coefficients for inter-observer differences in measured SUV_{mean}, SUV_{TF} ranged from 0.86 to 0.97, from 0.80 to 0.92, from (Table E2-E4) respectively. The value in SUV_{max} of patients with ILD (n=36) was 0.874 ($P < 0.001$). Thus, there were small inter-observer variances.

Comparison of Corrected SUV_{mean}, Corrected $SUV_{TF,}$ and CTD_{mean} on HRCT between NSCLC patients with and without ILD

$cSUV_{mean}$ was higher in NSCLC patients with than in those without ILD, in all locations except for both locations at the AA level, the ventral location at the TB level, and the ventral location at the RLPV level in the left lung (Table E5). $cSUV_{TF}$ was higher in all locations in NSCLC patients with than in those without ILD (Table E5). CTD_{mean} on HRCT was similar between NSCLC patients with and those without ILD at all locations (Table E6).

Comparison of Corrected SUV_{mean}, Corrected SUV_{TF}, Corrected SUV_{max}, and CTD_{mean} on HRCT between NSCLC patients with and those without postoperative ILD exacerbation

In NSCLC patients with postoperative ILD exacerbation, the value of $cSUV_{mean}$ in the right ventral and dorsal locations at the AA level, and the right ventral location at the TB level were higher than in those without postoperative AE (P = 0.01, P = 0.02, P = 0.02, respectively) (Table 2). Receiver operating characteristic (ROC) curve analysis at the 3 locations with a greater $cSUV_{mean}$ for NSCLC patients with AE also showed that the area under curve (AUC) for the right ventral location at the AA level in the right lung was greatest (AUC = 0.82), with an optimal cut-off value of 0.46. This cut-off value yielded a sensitivity of 75.0% and a specificity of 56.8% (Figure E1).

The value of $cSUV_{TF}$, $cSUV_{max}$, and CT_{mean} on HRCT showed no significant difference between the NSCLC patients with and those without postoperative AE at any of the locations (Tables 2, 3, E7).

Discussion

We investigated whether SUV in the less-affected lung parenchyma could predict postoperative AE of ILD in patients with NSCLC and ILD. The SUV_{mean} in NSCLC patients with postoperative AE of ILD was significantly higher than in those without AE, in several regions. ROC analysis showed that the AUC was greatest in the right ventral location at the AA level. Increased ^{18}F-FDG uptake in the dorsal and lower lung field has been shown to be associated with a gravitational effect and blood flow increase in some previous studies that used ^{18}F-FDG PET imaging (29, 30). Since respiratory movement in the lower lung field is generally regarded as larger than in the upper lung field, FDG accumulation tended to be overestimated in ^{18}F-FDG PET imaging in the lower lung field under free-breathing conditions. In an additional visual evaluation on HRCT before pulmonary surgery, with regard to the laterality of the interstitial lung shadow, the interstitial lung shadow in the group with postoperative AE was predominant in the right lung (P = 0.06). Therefore, while taking into account the factors influencing FDG accumulation, we consider that the higher SUV_{mean} in the ventral region of the upper lung field in those with postoperative AE than in those without AE is meaningful, and that SUV_{mean} measurement in normal-appearing ventral regions may be useful to predict postoperative AE.

On the other hand, SUV_{TF} was not significantly different between NSCLC patients with and those without postoperative AE. This may be because the mean CT value of ^{18}F-FDG-PET/CT in the right upper and middle lung field was higher in individuals with than in those without postoperative AE of ILD (data not

shown). In contrast, the mean CT value of HRCT obtained at peak-inspiration was similar between those with and those without postoperative AE of ILD. Since ^{18}F-FDG-PET/CT image data were obtained under free breathing conditions, the breathing level could not be kept constant. Data acquisition might sometimes have occurred during the expiratory phase on FDG-PET/CT in some patients. Moreover, the average CT value may be affected by the degree of pulmonary regional collapse as well as the increased blood flow. Therefore, SUV might be overcorrected based on regional CT density, due to the predominant focal collapse in NSCLC patients with postoperative AE of ILD, which could have obscured differences in SUV_{TF} between NSCLC patients with and those without postoperative AE of ILD. These results paradoxically imply that conventional CT obtained at peak-expiration may be useful for differentiating patients at increased risk of postoperative AE from those not at. As SUV_{TF} needs to be calculated by measuring the CT value of soft tissue and air (26), more time is required for imaging, which should be addressed as a drawback of SUV_{TF} calculation.

As in previously reports (18, 19), both SUV_{mean} and SUV_{TF} in the less-affected lung fields of NSCLC patients with ILD were significantly higher than in those patients without ILD. These results suggest that accumulation of ^{18}F-FDG in less-affected lung fields may reflect inflammatory conditions in the pulmonary interstitium, which cannot be visually detected with conventional HRCT. However, the mechanism underlying accumulation of ^{18}F-FDG in less-affected lung fields has remained incompletely understood. Disorders of the alveolar epithelium, migration of inflammatory cells, and release of inflammatory mediators were involved in the process of lung fibrosis in a bleomycin-hamster model (31). ^{18}F-FDG migrates into cells via glucose transporter 1 (GLUT-1), which was shown to be expressed in fibrocytes, bronchial epithelial cells, and inflammatory cells (32-34). These mechanisms may contribute to accumulation of ^{18}F-FDG in ILD. Accumulation of ^{18}F-FDG in less-affected lung fields in cases with ILDs would therefore show disease activity before morphological changes become detectable on HRCT.

There were several limitations in this study. First, this is a retrospective analysis with a small sample size. Therefore, the usefulness of SUV_{mean} measurement for less-affected regions in ventral upper lung field should be re-assessed in a larger number of cases in future. Second, regions where emphysematous changes exceeded 50% of the area were excluded from the target VOI setting in this study; however, the effect of emphysema could not be excluded completely. In a previous report, accumulation of ^{18}F-FDG in emphysema was elevated in chronic obstructive pulmonary disease patients as compared to healthy control (35).

In conclusion, the accumulation of ^{18}F-FDG in the less-affected lung fields may be able to predict postoperative AE of ILD in patients with NSCLC with ILD. If the value of SUV_{mean} in the less-affected lung field of the ventral region of the upper to middle lung field is high, patients should be monitored for AE of ILD after pulmonary surgery.

List Of Abbreviations

ILD: interstitial lung disease; AE: acute exacerbation; FDG: ^{18}F-flurodeoxyglucose; PET: positron emission tomography; CT: computed tomography; NSCLC: non-small cell lung cancer; VOI: volume-of-interest; SUV_{mean}: mean standardized uptake value; TF: tissue fraction; CTD_{mean}: mean computed tomography density; $cSUV_{mean}$: corrected SUV_{mean}; $cSUV_{TF}$: corrected SUV_{TF}; HRCT: high-resolution computed tomography; IPF: idiopathic pulmonary fibrosis; ECOG: Eastern Cooperative Oncology Group; KL-6: krebs von den lungen-6; UIP: usual interstitial pneumonia; AA: aortic arch; TB: tracheal bifurcation; RLPV: right lower pulmonary vein into the left atrium: NEMA: National Electrical Manufacturers Association; ROC: receiver operating characteristic; GLUT-1: glucose transporter 1; PAE: postoperative acute exacerbation; PS: performance status; ADC: adenocarcinoma; SQ: squamous cell carcinoma; AdSQ: adenosquamous cell carcinoma; Large: large cell carcinoma; %pred.: percent predicted; VC: vital capacity; FVC: forced vital capacity; TLC: total lung capacity; DL_{CO}: diffusing capacity of the lung for carbon monoxide; SP–D: surfactant protein–D; LDH: lactate dehydrogenase; CRP: C-reactive protein; AAV: aortic arch ventral; AAD: aortic arch dorsal; TBV: tracheal bifurcation ventral; TBD: tracheal bifurcation dorsal; RLPVV: right lower pulmonary vein ventral; RLPVD: right lower pulmonary vein dorsal.

Declarations

Ethics approval and consent to participate

This study was approved by our institutional review board (approved number: 29-190, November 2, 2017). The need to obtain informed patient consent was waived because of the retrospective nature of this research.

Consent for publication

Not applicable.

Availability of data and materials

All data generated or analysed during this study are included in this published article and its supplementary information files.

Competing interests

The authors declare no competing interests in association with this article.

Funding

None.

Authors' contributions

KF, YuN, TN, JH, and YaN conceived and designed the study. KF, YN, HN, AN-S, TN, MN, KK, HI, NN, and KM were involved in the analysis and interpretation of the clinical data; KF, YN, and YN were involved in the

drafting the manuscript.

Acknowledgment

We would like to thank Editage (www.editage.com) for English language editing.

References

1. King TE, Jr. Clinical advances in the diagnosis and therapy of the interstitial lung diseases. Am J Respir Crit Care Med 2005;172:268-279.
2. Travis WD, Costabel U, Hansell DM, King TE, Jr., Lynch DA, Nicholson AG, et al.An official american thoracic society/european respiratory society statement: Update of the international multidisciplinary classification of the idiopathic interstitial pneumonias. Am J Respir Crit Care Med 2013;188:733-748.
3. Hubbard R, Venn A, Lewis S, Britton J. Lung cancer and cryptogenic fibrosing alveolitis. A population-based cohort study. Am J Respir Crit Care Med 2000;161:5-8.
4. Archontogeorgis K, Steiropoulos P, Tzouvelekis A, Nena E, Bouros D. Lung cancer and interstitial lung diseases: a systematic review. Pulm Med 2012;2012:315918.
5. Harris JM, Johnston ID, Rudd R, Taylor AJ, Cullinan P. Cryptogenic fibrosing alveolitis and lung cancer: the BTS study. Thorax 2010;65:70-76.
6. Kenmotsu H, Naito T, Kimura M, Ono A, Shukuya T, Nakamura Y, et al.. The risk of cytotoxic chemotherapy-related exacerbation of interstitial lung disease with lung cancer. J Thorac Oncol 2011;6:1242-1246.
7. Ozawa Y, Akahori D, Koda K, Abe T, Hasegawa H, Matsui T, et al. Distinctive impact of pre-existing interstitial lung disease on the risk of chemotherapy-related lung injury in patients with lung cancer. Cancer Chemother Pharmacol 2016;77:1031-1038.
8. Minegishi Y, Takenaka K, Mizutani H, Sudoh J, Noro R, Okano T, et al. Exacerbation of idiopathic interstitial pneumonias associated with lung cancer therapy. Intern Med 2009;48:665-672.
9. Chiyo M, Sekine Y, Iwata T, Tatsumi K, Yasufuku K, Iyoda A, et al. Impact of interstitial lung disease on surgical morbidity and mortality for lung cancer: analyses of short-term and long-term outcomes. J Thorac Cardiovasc Surg 2003;126:1141-1146.
10. Okamoto T, Gotoh M, Masuya D, Nakashima T, Liu D, Kameyama K, et al. Clinical analysis of interstitial pneumonia after surgery for lung cancer. Jpn J Thorac Cardiovasc Surg 2004;52:323-329.
11. Koizumi K, Hirata T, Hirai K, Mikami I, Okada D, Yamagishi S, et al. Surgical treatment of lung cancer combined with interstitial pneumonia: the effect of surgical approach on postoperative acute exacerbation. Ann Thorac Cardiovasc Surg 2004;10:340-346.
12. Watanabe A, Kawaharada N, Higami T. Postoperative acute exacerbation of ipf after lung resection for primary lung cancer. Pulm Med 2011;2011:960316.
13. Sato T, Teramukai S, Kondo H, Watanabe A, Ebina M, Kishi K, et al. Impact and predictors of acute exacerbation of interstitial lung diseases after pulmonary resection for lung cancer. J Thorac

Cardiovasc Surgery 2014;147:1604-1611.

14. von Schulthess GK, Steinert HC, Hany TF. Integrated pet/ct: Current applications and future directions. Radiology 2006;238:405-422.
15. Nusair S, Rubinstein R, Freedman NM, Amir G, Bogot NR, et al. Positron emission tomography in interstitial lung disease. Respirology (Carlton, Vic) 2007;12:843-847.
16. Groves AM, Win T, Screaton NJ, Berovic M, Endozo R, Booth H, et al. Idiopathic pulmonary fibrosis and diffuse parenchymal lung disease: Implications from initial experience with 18F-FDG PET/CT. J Nucl Med 2009;50:538-545.
17. Uehara T, Takeno M, Hama M, Yoshimi R, Suda A, Ihata A, et al. Deep-inspiration breath-hold 18F-FDG-PET/CT is useful for assessment of connective tissue disease associated interstitial pneumonia. Mod Rheumatol 2016;26:121-127.
18. Win T, Thomas BA, Lambrou T, Hutton BF, Screaton NJ, Porter JC, et al. Areas of normal pulmonary parenchyma on hrct exhibit increased fdg pet signal in IPF patients. Eur J Nucl Med Mol Imaging 2014;41:337-342.
19. Nobashi T, Kubo T, Nakamoto Y, Handa T, Koyasu S, Ishimori T, et al. 18F-FDG uptake in less affected lung field provides prognostic stratification in patients with interstitial lung disease. J Nucl Med 2016;57:1899-1904.
20. Justet A, Laurent-Bellue A, Thabut G, Dieudonne A, Debray MP, Borie R, et al. [^{18}F]FDG PET/CT predicts progression-free survival in patients with idiopathic pulmonary fibrosis. Respir Res 2017;18:74.
21. Raghu G, Collard HR, Egan JJ, Martinez FJ, Behr J, Brown KK, et al. An official ATS/ERS/JRS/ALAT statement: idiopathic pulmonary fibrosis: evidence-based guidelines for diagnosis and management. Am J Respir Crit Care Med 2011;183:788-824.
22. Collard HR, Ryerson CJ, Corte TJ, Jenkins G, Kondoh Y, Lederer DJ, et al. Acute exacerbation of idiopathic pulmonary fibrosis. An International Working Group Report. Am J Respir Crit Care Med 2016;194:265-275.
23. Delbeke D, Coleman RE, Guiberteau MJ, Brown ML, Royal HD, Siegel BA, et al. Procedure guideline for tumor imaging with 18F-FDG PET/CT 1.0. J Nucl Med 2006;47:885-895.
24. Viglianti BL, Wong KK, Wimer SM, Parameswaran A, Nan B, Ky C, et al. Effect of hyperglycemia on brain and liver 18F-FDG standardized uptake value (FDG SUV) measured by quantitative positron emission tomography (PET) imaging. Biomed Pharmacother 2017;88:1038-1045.
25. Sprinz C, Altmayer S, Zanon M, Watte G, Irion K, Marchiori E, et al. Effects of blood glucose level on 18F-FDG uptake for PET/CT in normal organs: A systematic review. PLoS one 2018;13:e0193140.
26. Lambrou T, Groves AM, Erlandsson K, Screaton N, Endozo R, Win T, et al. The importance of correction for tissue fraction effects in lung PET: preliminary findings. Eur J Nucl Med Mol Imaging 2011;38:2238-2246.

27. Win T, Lambrou T, Hutton BF, Kayani I, Screaton NJ, Porter JC, et al. 18F-Fluorodeoxyglucose positron emission tomography pulmonary imaging in idiopathic pulmonary fibrosis is reproducible: Implications for future clinical trials. Eur J Nucl Med Mol Imaging 2012;39:521-528.
28. Okada M, Nakayama H, Okumura S, Daisaki H, Adachi S, Yoshimura M, et al. Multicenter analysis of high-resolution computed tomography and positron emission tomography/computed tomography findings to choose therapeutic strategies for clinical stage IA lung adenocarcinoma. Jthoracic and cardiovascular surgery 2011;141:1384-1391.
29. Miyauchi T, Wahl RL. Regional 2-[18F]fluoro-2-deoxy-d-glucose uptake varies in normal lung. Eur J Nucl Med 1996;23:517-523.
30. Inoue K, Okada K, Taki Y, Goto R, Kinomura S, Fukuda H. (18)FDG uptake associated with CT density on PET/CT in lungs with and without chronic interstitial lung diseases. Ann Nucl Med 2009;23:277-281.
31. Iyer SN, Hyde DM, Giri SN. Anti-inflammatory effect of pirfenidone in the bleomycin-hamster model of lung inflammation. Inflammation 2000;24:477-491.
32. Mamchaoui K, Makhloufi Y, Saumon G. Glucose transporter gene expression in freshly isolated and cultured rat pneumocytes. Acta Physiol Scand 2002;175:19-24.
33. Pezzulo AA, Gutierrez J, Duschner KS, McConnell KS, Taft PJ, Ernst SE, et al. Glucose depletion in the airway surface liquid is essential for sterility of the airways. PLoS one 2011;6:e16166.
34. El-Chemaly S, Malide D, Yao J, Nathan SD, Rosas IO, Gahl WA, et al. Glucose transporter-1 distribution in fibrotic lung disease: Association with [^{18}F]-2-fluoro-2-deoxyglucose-PET scan uptake, inflammation, and neovascularization. Chest 2013;143:1685-1691.
35. Subramanian DR, Jenkins L, Edgar R, Quraishi N, Stockley RA, Parr DG. Assessment of pulmonary neutrophilic inflammation in emphysema by quantitative positron emission tomography. Am J Respir Crit Care Med 2012;186:1125-1132.

Tables

Table 1. The characteristics of the non-small cell lung cancer (NSCLC) patients with or without postoperative acute exacerbation of interstitial lung disease.

	PAE (+) n = 8	PAE (–) n = 28	P
Age	71 (66–77.3)	73.5 (69.3–77)	0.54
Sex (M/F)	8/0	25/3	0.21
Smoking (Current + Former/Never)	8/0	27/1	0.47
Pack–year	49 (40.5–73.3)	51 (38.5–76.5)	0.79
ECOG PS (0–1/2)	7/1	28/0	0.08
Histology (ADC/SQ/AdSq/Large)	2/4/1/1	14/13/1/0	0.19
Surgical procedure (Wedge/resection/Segmentectomy/ Lobectomy/Bilobectomy)	0/2/5/1	4/3/21/0	0.11
Stage (□/□/□/□□	6/0/1/1	20/4/4/0	0.17
UIP/non-UIP	4/4	12/16	0.72
VC (L)	3.08 (2.58–3.38)	3.03 (2.64–3.60)	0.70
%VC (%)	94.4 (84.0–105.9)	98.3 (82.5–112.2)	0.51
FVC (L)	3.00 (2.55–3.39)	3.04 (2.68–3.62)	0.80
%FVC (%)	94.9 (84.2–104.4)	98.3 (81.8–113.3)	0.48
TLC (L) PAE+ = 7, PAE– = 26	4.81 (4.35–5.07)	4.94 (4.23–5.43)	0.71
%TLC (%) PAE+ = 7, PAE– = 26	87.5 (77.4–94.3)	91.2 (79.8–98.1)	0.41
DLco (ml/min/mmHg) PAE+ = 7, PAE– = 26	11.99 (9.81–15.16)	10.94 (8.88–14.23)	0.39
%DLco (%) PAE+ = 7, PAE– = 26	85.8 (50.1–105.6)	73.4 (61.23–93.18)	0.66
KL–6 PAE+ = 8, PAE– = 23	476.8 (349.0–1287.9)	461.0 (308.8–648)	0.46
SP–D PAE+ = 7, PAE– = 20	185 (105–314)	108 (51.1–147.0)	0.03
LDH	203 (189–267.3)	199.5 (171.5–224)	0.61
CRP	0.28 (0.12–0.32)	0.19 (0.12–0.49)	0.92

Data are presented as the number or median (interquartile range).

Abbreviations: PAE: postoperative acute exacerbation; NSCLC: non–small cell lung cancer; ILD: interstitial lung disease; ECOG: Eastern Cooperative Oncology Group; PS: performance status; ADC: adenocarcinoma; SQ: squamous cell carcinoma; AdSQ: adenosquamous cell carcinoma; Large: large cell carcinoma; %pred.: percent predicted; VC: vital capacity; FVC: forced vital capacity; TLC: total lung capacity; DL_{CO}: diffusing capacity of the lung for carbon monoxide; KL-6: Krebs von den Lungen–6; SP–D: surfactant protein–D; LDH: lactate dehydrogenase; CRP: C-reactive protein.

Table 2. Comparison of correct SUV_{mean} and SUV_{TF} between non-small cell lung cancer (NSCLC) patients with or without postoperative acute exacerbation of interstitial lung disease (ILD).

		Correct SUV_{mean}			Correct SUV_{TF}		
		PAE+ median	PAE– median	P	PAE+ median	PAE– median	P
Right lung	RAV PAE+ = 8, PAE– = 22	0.51 (0.43–0.63)	0.40 (0.29–0.44)	0.01	2.56 (2.06–2.77)	2.25 (1.97–2.47)	0.21
	RAD PAE+ = 8, PAE– = 22	0.56 (0.48–0.62)	0.45 (0.36–0.50)	0.02	2.59 (2.35–2.78)	2.20 (1.88–2.62)	0.21
	RBV PAE+ = 8, PAE– = 26	0.50 (0.36–0.58)	0.36 (0.29–0.41)	0.02	2.54 (2.23–2.86)	2.24 (1.90–2.45)	0.11
	RBD PAE+ = 7, PAE– = 22	0.55 (0.48–0.57)	0.45 (0.41–0.53)	0.28	2.40 (2.29–2.76)	2.20 (1.88–2.80)	0.52
	RLPVV PAE+ = 8, PAE– = 27	0.44 (0.37–0.51)	0.35 (0.28–0.45)	0.16	2.50 (2.00–2.81)	2.22 (1.87–2.56)	0.28
	RLPVD PAE+ = 7, PAE– = 26	0.57 (0.47–0.77)	0.53 (0.43–0.62)	0.37	2.37 (2.10–2.57)	2.45 (2.08–2.66)	0.66
Left lung	LAV PAE+ = 7, PAE– = 22	0.41 (0.35–0.50)	0.39 (0.32–0.43)	0.49	2.06 (1.86–2.24)	2.33 (1.91–2.65)	0.32
	LAD PAE+ = 7, PAE– = 22	0.49 (0.41–0.56)	0.44 (0.36–0.47)	0.26	2.23 (1.81–2.61)	2.23 (1.97–2.46)	0.98
	LBV PAE+ = 8, PAE– = 26	0.45 (0.37–0.53)	0.38 (0.32–0.41)	0.95	2.41 (2.24–2.74)	2.28 (1.91–2.54)	0.23
	LBD PAE+ = 8, PAE– = 27	0.55 (0.43–0.63)	0.47 (0.39–0.52)	0.15	2.29 (1.86–2.54)	2.28 (1.97–2.56)	0.95
	LLPVV PAE+ = 7, PAE– = 18	0.44 (0.41–0.62)	0.32 (0.36–0.39)	0.06	2.34 (1.75–2.41)	2.16 (1.82–2.50)	0.63
	LLPVD PAE+ = 7, PAE– = 23	0.63 (0.55–0.71)	0.51 (0.42–0.59)	0.11	2.26 (2.17–2.57)	2.18 (1.95–2.44)	0.42

Data are presented as the number or median (interquartile range). Abbreviations: SUV: standardized uptake value; TF: tissue fraction; NSCLC: non–small cell lung cancer; ILD: interstitial lung disease; PAE: postoperative acute exacerbation; AAV: aortic arch ventral; AAD: aortic arch dorsal; TBV: tracheal bifurcation ventral; TBD: tracheal bifurcation dorsal; RLPVV: right lower pulmonary vein ventral; RLPVD: right lower pulmonary vein dorsal.

Table 3. Comparison of mean computed tomography density of target volume-of-interest (VOI) in high-resolution computed tomography (HRCT) between non-small cell lung cancer (NSCLC) patients with and without postoperative acute exacerbation of interstitial lung disease (ILD).

		CTD_{mean}		
		ILD+ median	ILD– median	P
Right lung	AAV PAE+ = 8, PAE– = 22	–877.0 (–883.2 to –830.2)	–878.6 (–905.2 to –868.0)	0.25
	AAD PAE+ = 8, PAE– = 22	–822.3 (–889.0 to –808.2)	–857.6 (–878.1 to –834.3)	0.13
	TBV PAE+ = 8, PAE– = 26	–878.5 (–894.2 to –867.2)	–884.4 (–912.9 to –866.6)	0.35
	TBD PAE+ = 7, PAE– = 22	–872.2 (–877.1 to –854.7)	–855.2 (–876.1 to –837.6)	0.56
	RLPVV PAE+ = 8, PAE– = 27	–896.6 (–908.1–-883.7)	–884.5 (–919.1 to –871.6)	0.95
	RLPVD PAE+ = 7, PAE– = 26	–841.1 (–871.7 to –813.7)	–857.3 (–882.7 to –841.7)	0.23
Left lung	AAV PAE+ = 7, PAE– = 22	–866.4 (–903.0 to –819.2)	–882.6 (–911.1 to –862.9)	0.16
	AAD PAE+ = 7, PAE– = 22	–865.4 (–893.8 to –829.0)	–868.6 (–891.3 to –838.4)	0.94
	TBV PAE+ = 8, PAE– = 26	–882.2 (–906.7 to –855.9)	–884.7 (–905.9 to –873.9)	0.53
	TBD PAE+ = 8, PAE– = 27	–866.0 (–887.5 to –838.1)	–871.3 (–898.4 to –847.5)	0.49
	RLPVV PAE+ = 7, PAE– = 18	–880.0 (–895.0 to –870.6)	–882.5 (–898.0 to –853.3)	0.90
	RLPVD PAE+ = 7, PAE– = 23	–846.4 (–886.0 to –837.4)	–852.6 (–874.8 to –812.7)	1.00

Data are presented as the number or median (interquartile range).

Abbreviations: CTD_{mean}: mean computed tomography density; VOI: volume of interest; HRCT: high-resolution computed tomography; TF: tissue fraction; NSCLC: non–small cell lung cancer; ILD: interstitial lung disease; PAE: postoperative acute exacerbation; RAV: right aortic arch ventral; RAD: right aortic arch dorsal; LAV: left aortic arch ventral; LAD: left aortic arch dorsal, RBV: right bronchial bifurcation ventral; RBD: right bronchial bifurcation dorsal; LBV: left bifurcation ventral; LBD: left bronchial bifurcation dorsal; RLPVV: right lower pulmonary vein ventral; RLPVD: right lower pulmonary vein dorsal; LLPVV: left lower pulmonary vein ventral; LLPVD: left lower pulmonary vein dorsal.

Figures

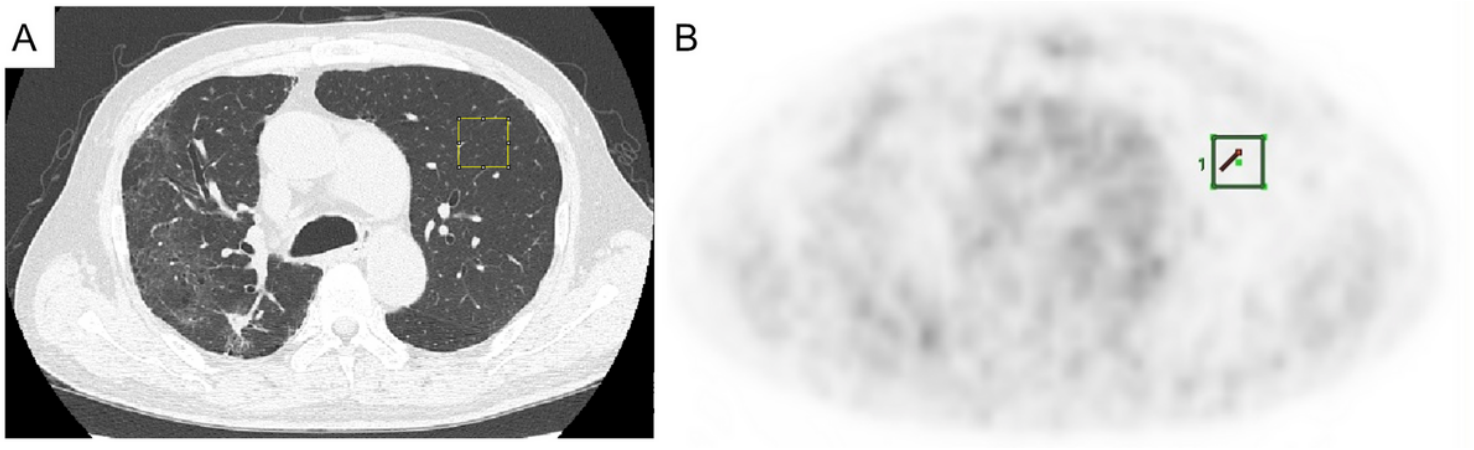

Figure 1

Typical images of volumes-of-interest (VOIs) for measuring SUVmean and CTmean. (A) A cubic VOI of 18 cm3 was manually located on the less-affected lung field of a high-resolution computed tomography image. (B) The corresponding VOI was manually located on a positron-emission tomography image.

Supplementary Files

This is a list of supplementary files associated with this preprint. Click to download.

- FigureE1.pptx